Lehrer, S. S., & Leavis, P. C. (1978) *Methods Enzymol. 49*, 222–236.
Lewis, S. D., Johnson, F. A., & Shafer, J. A. (1976) *Biochemistry 15*, 5009–5017.
Lottspeich, F., Kellermann, J., Henschen, A., Foertsch, B., & Müller-Esterl, W. (1985) *Eur. J. Biochem. 152*, 307–314.
Lowe, G., & Whitworth, A. S. (1974) *Biochem. J. 141*, 503–515.
Müller-Esterl, W., Fritz, H., Machleidt, W., Ritonja, A., Brzin, J., Kotnik, M., Turk, V., Kellermann, J., & Lottspeich, F. (1985) *FEBS Lett. 182*, 310–314.
Nicklin, M. J. H., & Barrett, A. J. (1984) *Biochem. J. 223*, 245–253.
Nordenman, B., & Björk, I. (1978) *Biochemistry 17*, 3339–3344.
Ohkubo, I., Kurachi, K., Takasawa, T., Shiokawa, H., & Sasaki, M. 1984) *Biochemistry 23*, 5691–5697.
Ornstein, L. (1964) *Ann. N.Y. Acad. Sci. 121*, 321–349.
Roberts, D. D., Lewis, S. D., Ballou, D. P., Olson, S. T., & Shafer, J. A. (1986) *Biochemistry 25*, 5595–5601.
Schwabe, C., Anastasi, A., Crow, H., McDonald, J. K., & Barrett, A. J. (1984) *Biochem. J. 217*, 813–817.
Sluyterman, L. A. AE., & De Graaf, M. J. M. (1970) *Biochim. Biophys. Acta 200*, 595–597.
Smith, D. J., Maggio, E. T., & Kenyon, G. L. (1975) *Biochemistry 14*, 766–771.
Spande, T. F., & Witkop, B. (1967) *Methods Enzymol. 11*, 498–506.
Strickland, E. H. (1974) *CRC Crit. Rev. Biochem. 2*, 113–175.
Sueyoshi, T., Enjyoji, K., Shimada, T., Kato, H., Iwanaga, S., Bando, Y., Kominami, E., & Kaunuma, N. (1985) *FEBS Lett. 182*, 193–195.
Takeda, A., Kobayashi, S., Kaji, H., Aoki, Y., & Samejima, T. (1986) *J. Biochem. (Tokyo) 99*, 785–791.
Turk, V., Brzin, J., Longer, M., Ritonja, A., & Eropkin, M. (1983) *Hoppe-Seyler's Z. Physiol. Chem. 364*, 1487–1496.
Weber, K., & Osborn, M. (1969) *J. Biol. Chem. 244*, 4406–4412.

Mechanism of Binding of Horse Liver Alcohol Dehydrogenase and Nicotinamide Adenine Dinucleotide†

V. Chandra Sekhar and Bryce V. Plapp*
Department of Biochemistry, The University of Iowa, Iowa City, Iowa 52242
Received January 4, 1988; Revised Manuscript Received March 3, 1988

ABSTRACT: The binding of NAD^+ to liver alcohol dehydrogenase was studied by stopped-flow techniques in the pH range from 6.1 to 10.9 at 25 °C. Varying the concentrations of NAD^+ and a substrate analogue used to trap the enzyme–NAD^+ complex gave saturation kinetics. The same maximum rate constants were obtained with or without the trapping agent and by following the reaction with protein fluorescence or absorbance of a ternary complex. The data fit a mechanism with diffusion-controlled association of enzyme and NAD^+, followed by an isomerization with a forward rate constant of 500 s^{-1} at pH 8: $E \rightleftharpoons E\text{–}NAD^+ \rightleftharpoons {}^*E\text{–}NAD^+$. The isomerization may be related to the conformational change determined by X-ray crystallography of free enzyme and enzyme–coenzyme complexes. Overall bimolecular rate constants for NAD^+ binding show a bell-shaped pH dependence with apparent pK values at 6.9 and 9.0. Acetimidylation of ϵ-amino groups shifts the upper pK to a value of 11 or higher, suggesting that Lys-228 is responsible for the pK of 9.0. Formation of the enzyme–imidazole complex abolishes the pK value of 6.9, suggesting that a hydrogen-bonded system extending from the zinc-bound water to His-51 is responsible for this pK value. The rates of isomerization of $E\text{–}NAD^+$ and of pyrazole binding were maximal at pH below a pK of about 8, which is attributable to the hydrogen-bonded system. Acetimidylation of lysines or displacement of zinc–water with imidazole had little effect on the rate of isomerization of the $E\text{–}NAD^+$ complex. Rate constants from a computer simulation suggest that the isomerization partially controls the transient phase of 1-propanol oxidation.

The three-dimensional structures of horse liver alcohol dehydrogenase (EC 1.1.1.1) and its complexes show that the two domains of each subunit move closer together upon forming complexes with NAD^+ and pyrazole (Eklund et al., 1982a), NAD^+ and trifluoroethanol (Plapp et al., 1978), NAD^+ and *p*-bromobenzyl alcohol (Eklund et al., 1982b), and NADH and dimethyl sulfoxide (Eklund et al., 1981). This conformational change is thought to be important for catalysis because residues in the active site are repositioned and water is excluded from the active site (Eklund & Brändén, 1987; Colonna-Cesari et al., 1986; Eklund et al., 1984). Identifying the step, or steps, in the mechanism where the conformation changes and assessing the factors that control the change are the subject of this work.

Steady-state results suggest that the enzyme–NAD^+ complex isomerizes, as the rate constant for dissociation of NAD^+ calculated on the assumption of the ordered bi bi mechanism is 2-fold less than the turnover number for the reduction of acetaldehyde (Wratten & Cleland, 1963; Plapp et al., 1986). Pressure relaxation studies on the enzyme–NAD^+ complex have given preliminary estimates of the rates of isomerization

†This work was supported by Grant AA00279 from the National Institute on Alcohol Abuse and Alcoholism, U.S. Public Health Service.

0006-2960/88/0427-5082$01.50/0

and suggest that isomerization can be rate limiting in turnover (Coates et al., 1977; Hardman, 1981). Quenching of protein fluorescence during NAD^+ binding, and the pH dependence thereof, can also be explained by a conformational change of free and complexed enzyme (Wolfe et al., 1977; Parker et al., 1978). The results from the present study support the conclusion that the enzyme–NAD^+ complex isomerizes and suggest roles for Lys-228 and His-51 in the binding reaction.

Experimental Procedures

All chemicals were of reagent grade unless specified otherwise. NAD^+ (lithium salt, Boehringer-Mannheim, grade I), 2,2,2-trifluoroethanol (Aldrich, Gold Label), and ethyl acetimidate hydrochloride (Eastman Kodak) were used as received. 1-Propanol was distilled prior to use. Crystalline horse liver alcohol dehydrogenase (Boehringer-Mannheim) was dissolved in a high-salt buffer and freed of ethanol by gel filtration on a column of Sephadex G-50 with 1 mM sodium phosphate buffer, pH 8. Protein concentration was determined with $\epsilon_{280} = 36.4\ mM^{-1}\ cm^{-1}$. The normality of enzyme active sites was titrated with NAD–pyrazole ($\epsilon_{300} = 7.2\ mM^{-1}\ cm^{-1}$; Theorell & Yonetani, 1963). Solutions of NAD^+ and substrates or substrate analogues were prepared just before doing the kinetic studies. Concentrations of NAD^+ were checked with $\epsilon_{260} = 18\ mM^{-1}\ cm^{-1}$. Acetimidylated enzyme was prepared and purified as previously described (Hennecke & Plapp, 1983). Enzyme (about 20 μN) complexed with imidazole at the catalytic zinc was formed with 30 mM imidazole for reactions at pH 7 and above and 150 mM imidazole at pH 6, so as to keep the concentration of unprotonated ligand at 5–10 times the K_d value (Sigman, 1967). Buffers for pH dependency studies were prepared at 0.2 ionic strength and diluted with an equal volume of enzyme solution in the experiment; 20 mM $Na_4P_2O_7$ was adjusted to the desired pH with H_3PO_4 and ionic strength with NaH_2PO_4 and Na_2HPO_4 for pH 5.5–9.0, and 66 mM Na_2HPO_4–glycine buffers (Dalziel, 1963) were used above pH 9.0.

pH was measured with a Radiometer Model 26 pH meter. Spectra were recorded on a Cary 118 spectrophotometer. All the transient kinetics were done at 25 °C. Two stopped-flow instruments were used: a Durrum-Gibson Model 110 instrument and a custom instrument designed by Dr. David P. Ballou with a Durrum-Gibson monochromator and a Kinetic Instruments rapid-mixing device, interfaced with an IBM PC/AT computer. The dead times for these instruments were determined by studying the kinetics of ascorbic acid (0.3–35 mM) reaction (ΔA_{524}) with 25 μM 2,6-dichlorophenolindophenol in pH 3 phthalate buffer and were found to be about 3.5 and 1.3 ms, respectively (Tonomura et al., 1978). Apparent rate constants were a linear function of the concentration of ascorbate up to 330 s^{-1} on the Durrum-Gibson and up to 750 s^{-1} on the Kinetic Instruments stopped-flow spectrophotometers. Computer programs (Dunn et al., 1979) adapted to run on a Vax 11/780 or from On-Line Instruments Systems (Jefferson, GA) were used for data acquisition and reduction.

Reactions were initiated by mixing the enzyme in low ionic strength pH 8 buffer from one drive syringe and NAD^+ and substrate or substrate analogue in 0.2 ionic strength buffer of desired pH from the other syringe. This procedure was used because the enzyme was most stable at pH 8 and an ionic strength of 0.1 in the reaction mixtures was desired. The reactions were complete in less than 1 s, and the enzyme undergoes no significant irreversible inactivation during this time, even at pH 11 (Andersson et al., 1981a). The pH of the buffer containing NAD^+ before mixing with enzyme was the same as the pH of the completed reaction. Enzyme concentration in the reactions was about 10 μN when the absorbance mode was used and about 3 μN when the fluorescence mode was used. NAD^+ concentration was varied from 0.1 to 1.0 mM for the reactions of enzyme with NAD^+ and pyrazole but was kept saturating (2.0–8.0 mM) for reactions with propanol. Formation of complexes of enzyme with NAD^+ and pyrazole (varied from 0.25 to 25 mM) or hydroxylamine hydrochloride (10–100 mM) was followed either by the increase in absorbance of ternary complex at 300 nm or by the decrease in protein fluorescence (λ_{ex} = 290 nm and λ_{em} > 315 nm). The reactions of enzyme with NAD^+ in the absence of any substrate analogue and in the presence of trifluoroethanol (0.5–10 mM) were followed by the decrease in protein fluorescence during the reaction. Alcohol oxidation was monitored by the increase in absorbance ($\epsilon = 5.5\ mM^{-1}\ cm^{-1}$) of NADH at 328 nm, which is the isosbestic point for free and enzyme-bound forms of NADH (Theorell & Bonnichsen, 1951). Concentrations of NAD^+ and substrate or substrate analogue were kept in excess over enzyme concentration to ensure pseudo-first-order reactions. Data for ternary complex formation were fitted by a first-order process, whereas the formation of NADH during alcohol oxidation was fitted by an equation for an exponential process followed by a steady state. Apparent first-order rate constants for the reaction of enzyme with NAD^+ and substrate analogue were fitted by eq 1 (I = substrate analogue) with the SEQUEN program (Cleland, 1979). A nonlinear least-squares program (C. M. Metzler, The Upjohn Co., Kalamazoo, MI) was used to compute the pK values from the pH dependence of kinetic constants. The kinetic simulation program KINSIM (Barshop et al., 1983) and an automatic regression routine, FITSIM (Zimmerle et al., 1987), were used to obtain rate constants from progress curves.

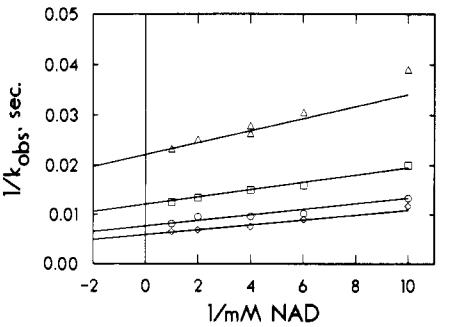

FIGURE 1: Dependence of observed rate constants for formation of the native enzyme–NAD–pyrazole complex on concentration of NAD^+ and pyrazole. Concentrations of pyrazole were 0.5 (△), 1.0 (□), 1.75 (○), and 2.5 mM (◇). The buffer was 0.1 ionic strength sodium pyrophosphate–phosphate, pH 8.0, at 25 °C. Lines are calculated with eq 1 with K_{NAD} = 0.17 mM, K_{ia} = 43 μM, K_{pyz} = 5.5 mM, and k = 540 s^{-1}. Since the lines are almost parallel, the data could be fitted, slightly less well, by the PINGPONG equation (Cleland, 1979).

$$k_{obsd} = \frac{k[NAD][I]}{K_{ia}K_I + K_{NAD}[I] + K_I[NAD] + [NAD][I]} \quad (1)$$

Results

Limiting Rate in Binding NAD^+. The data in Figure 1 show that the rate of binding of NAD^+ to horse liver alcohol dehydrogenase in the presence of pyrazole was saturable with respect to the concentrations of NAD^+ and pyrazole. Previous work showed saturation kinetics when the concentration of only one ligand was varied (Plapp et al., 1973; Gilleland & Shore, 1970). We also found that pyrazole concentrations of 10 mM or higher were inhibitory at pH 8 and 25 °C. Steady-state kinetics indicate that the mechanism of alcohol oxidation is

Table I: Rate Constants for Limiting Reaction and NAD^+ Association for Native Enzyme at pH 8.0 and 25 °C[a]

substrate analogue	signal	k (s^{-1})	k/K_{NAD} (μM^{-1} s^{-1})	k/K_I (M^{-1} s^{-1})
pyrazole	A	540	3.1[b]	9.9×10^4
pyrazole	F	430	1.5	[c]
pyrazole[d]	A	460	0.4	3.3×10^4
hydroxylamine[e]	A	430	0.5	4.8×10^3
trifluoroethanol	F	490	1.6	1.4×10^5

[a] A = absorbance of ternary complex at 300 nm, F = protein fluorescence (λ_{ex} = 290 nm and λ_{em} > 315 nm). The rate constants were obtained from the fit of apparent pseudo-first-order rate constants to eq 1. Standard errors for specific rate constants were less than 20%. [b] This value had an error of 30%. [c] This value was not accurately determined because the concentrations of pyrazole used for this experiment were not subsaturating. [d] For this experiment, native enzyme was mixed with 30 mM imidazole to replace the water molecule bound to zinc, which probably caused the 5-fold reduction in k/K_{NAD}. [e] NH_2OH·HCl was used, and the chloride ion binds to free enzyme, decreasing k/K_{NAD} (Oldén & Pettersson, 1982).

predominantly ordered (Wratten & Cleland, 1963; Dalziel & Dickinson, 1966) and that pyrazole binds after NAD^+ (Theorell et al., 1969). Thus, apparent pseudo-first-order rate constants for the formation of enzyme–NAD–pyrazole complex were fitted to eq 1 for a sequential bi mechanism (Figure 1).

The limiting rate constant observed for the formation of the ternary complex can be explained by the mechanism shown in Scheme I. At saturating concentrations of NAD^+ and pyrazole, the observed rate constant reaches the limiting value of k_2, corresponding to isomerization of enzyme–NAD^+ complex. Pyrazole reacts with the second enzyme–NAD^+ complex with no detectable limiting rate (Frolich et al., 1978) and traps the complex by forming a covalent bond to the NAD^+ (Eklund et al., 1982b). Pyrazole binds weakly to free enzyme (Sigman 1967).

Scheme I

$$E \underset{k_{-1}}{\overset{k_1,\ NAD^+}{\rightleftharpoons}} E\text{–}NAD^+ \underset{k_{-2}}{\overset{k_2}{\rightleftharpoons}} {}^*E\text{–}NAD^+ \underset{k_{-3}}{\overset{k_3,\ pyz}{\rightleftharpoons}} \text{E–NAD–pyrazole}$$

In order to support this mechanism and eliminate mechanisms that would involve a rate-limiting reaction of a complex with pyrazole (e.g., dissociation of enzyme–pyrazole or isomerization of enzyme–NAD^+–pyrazole complex), NAD^+ binding was studied in the presence of other agents that form a stable ternary complex. The results in Table I show that the same limiting rate is obtained in the presence of hydroxylamine or trifluoroethanol. Moreover, the same limiting rate is apparent when the reaction is followed by monitoring changes in either protein fluorescence or absorbance of ternary complex at 300 nm.

Furthermore, kinetics of NAD^+ association were investigated in the absence of any substrate analogue. This reaction was studied at pH 9 and above as both association and dissociation rate constants for NAD^+ are known to be slower at higher pH (Detraglia et al., 1977; Kvassman & Pettersson, 1979). Figure 2 shows that apparent rate constants for NAD^+ binding are a function of NAD^+ concentration at pH 10. Saturation kinetics were evident, and the rate constant at infinite NAD^+ concentration could correspond to the isomerization rate constant k_2, as k_{-2} is small. The limiting rate constant obtained by this method is 30–40% larger than the value observed from absorbance in the presence of pyrazole. At low pH, NAD^+ association and dissociation rate constants are large, and the formation of *E–NAD^+ complex becomes a relaxation process in the absence of substrate analogues.

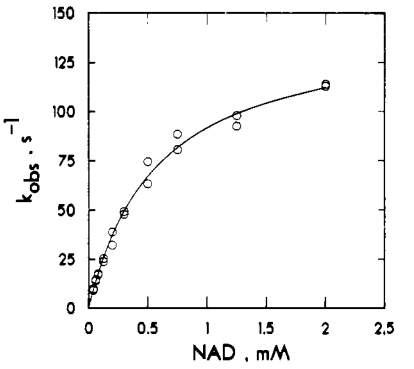

FIGURE 2: Dependence of observed rate constants for NAD^+ binding to native enzyme upon NAD^+ concentration at 25 °C and pH 10. First-order rate constants for protein fluorescence quenching (λ_{ex} = 290 nm, λ_{em} > 315 nm) upon mixing 8 μN native enzyme (syringe 1) with 0.1–4.0 mM NAD^+ in phosphate–glycine buffer of pH 10 (syringe 2) were fitted to the expression $k_{obsd} = k_{-2} + k_2/(1 + K_d/[NAD^+])$ with values of k_{-2} = 0.5 s^{-1} (fixed), k_2 = 145 s^{-1}, and K_d = 0.58 mM for the mechanism

$$E \overset{K_d}{\rightleftharpoons} E\text{–}NAD^+ \underset{k_{-2}}{\overset{k_2}{\rightleftharpoons}} {}^*E\text{–}NAD^+$$

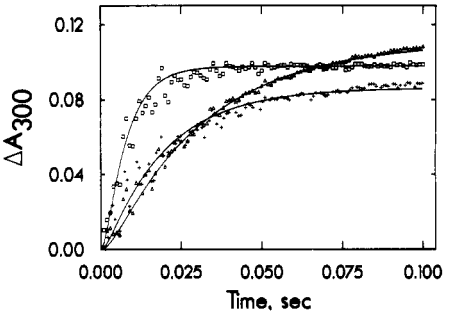

FIGURE 3: Kinetics of formation of ternary E–NAD–pyrazole complex. Points are experimental, and lines are simulated progress curves from the FITSIM program. Estimated rate constants are listed in Table II. Native enzyme (8 μN) at pH 8.0 reacted with 0.1 mM NAD^+ and 0.5 mM pyrazole (△), 0.5 mM NAD^+ and 1.75 mM pyrazole (□), and 1.0 mM NAD^+ and 0.5 mM pyrazole (+).

Table II: Rate Constants for the Reaction of Native Enzyme with NAD^+ and Pyrazole[a]

k_1 (μM^{-1} s^{-1})	k_{-1} (s^{-1})	k_2 (s^{-1})	k_{-2} (s^{-1})	k_3 (mM^{-1} s^{-1})
60	14000	500	120	140

[a] These rate constants were estimated by fitting the data obtained at pH 8.0 on the stopped-flow instrument to the computer simulation regression program FITSIM with the mechanism give in Scheme I. The value for k_{-3} was assumed to be 0.03 s^{-1}. Standard errors for the estimated values of rate constants were less than 25%.

Thus, the apparent rate constants are out of the range of the stopped-flow instrument, and no attempt was made to study kinetics of this reaction below pH 9.0.

We also used the kinetic simulation programs KINSIM/FITSIM to fit the progress curves for the formation of E–NAD–pyrazole. Figure 3 shows that the data were well simulated with Scheme I for the formation of E–NAD–pyrazole; the estimated rate constants are presented in Table II. The simulation was also applied to other possible mechanisms that could explain the kinetics. In general, good fits were obtained if a three-step mechanism was used. A mechanism (Scheme II) with a dead-end enzyme–NAD^+ complex that could not react with pyrazole gave equal values for k_1 and k_2, with the limiting rate corresponding to k_{-1}. This mechanism would predict that the observed amplitude would decrease to 50% of the maximum when the concentrations of NAD^+ were saturating. Since the amplitude was at least 83% of the ex-

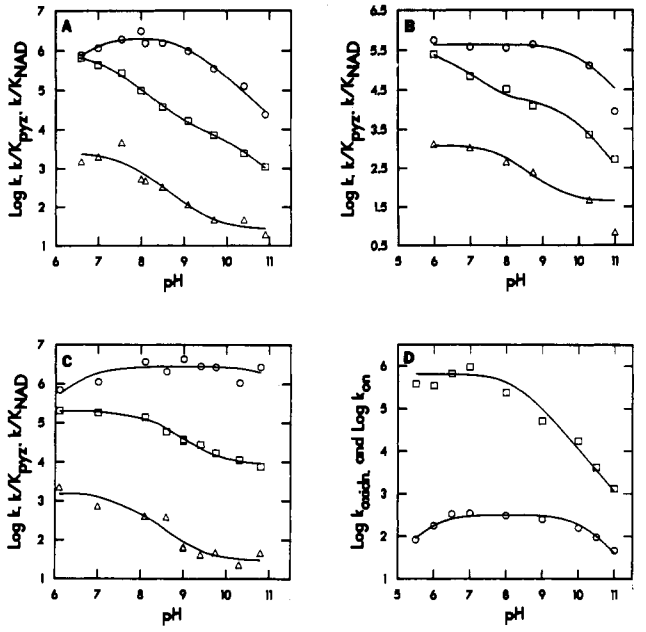

FIGURE 4: pH dependence of kinetic constants for various reactions. Lines were calculated with the kinetic constants and expressions given in Table III. (A) Reaction of native enzyme with NAD^+ and pyrazole: k (△), k/K_{NAD} (○), and k/K_{pyz} (□) were determined by the fit of observed rate constants to eq 1. (B) Reaction of NAD^+ and pyrazole with enzyme that has imidazole bound to catalytic zinc: k (△), k/K_{NAD} (○), and k/K_{pyz} (□). (C) Reaction of acetimidylated enzyme with NAD^+ and pyrazole: k (△), k/K_{NAD} (○), and k/K_{pyz} (□). (D) Transient oxidation of 1-propanol by NAD^+ and native enzyme: k_{oxidn} (○) and k_{on} (k/K_m for propanol) (□). The kinetic constants at each pH were determined from the HYPER program (Cleland, 1979).

pected value, after correction for the reaction occurring in the dead time of the instrument, this mechanism is not likely.

Scheme II

$$*E\text{–}NAD^+ \overset{k_1,\ NAD^+}{\underset{k_{-1}}{\rightleftharpoons}} E \overset{k_2,\ NAD^+}{\underset{k_{-2}}{\rightleftharpoons}} E\text{–}NAD^+ \overset{k_3,\ pyz}{\underset{k_{-3}}{\rightleftharpoons}} E\text{–}NAD\text{–}pyrazole$$

Another mechanism (Scheme III) for which good simulations were obtained has two different forms of enzyme, only one of which binds NAD^+. In this case, *E would be the predominant form of apoenzyme, according to values obtained from the simulations (pH 8; k_1, 10000 s^{-1}; k_{-1}, 200 s^{-1}; k_{-2}, 70 s^{-1}). This is an interesting mechanism, as Parker et al. (1978) had suggested that conformational change of free enzyme (e.g., *E → E), favored above a pK of 9.8, could explain protein fluorescence titrations. However, amplitudes for reactions at saturating NAD^+ and pyrazole concentrations did not decrease at high pH, which suggests that any such isomerization is not kinetically limiting. Furthermore, there is no direct evidence for different conformers of apoenzyme, such as from X-ray crystallography, which has provided only one "open" and one "closed" form (Eklund & Brändén, 1987). Even complexes with NAD^+ fragments or analogues retain the open conformation. Finally, with this mechanism, the rate constant calculated from steady-state kinetic data for dissociation of NAD^+ should be 35-fold smaller than the turnover number with NADH and acetaldehyde at pH 8 and 25 °C, whereas the numbers agree within a factor of 2 (Plapp et al., 1986).

Scheme III

$$*E \overset{k_1}{\underset{k_{-1}}{\rightleftharpoons}} E \overset{k_2,\ NAD^+}{\underset{k_{-2}}{\rightleftharpoons}} E\text{–}NAD^+ \overset{k_3,\ pyz}{\underset{k_{-3}}{\rightleftharpoons}} E\text{–}NAD\text{–}pyrazole$$

Scheme IV

$$\begin{array}{ccccc} H_2E & \overset{K_a}{\rightleftharpoons} & HE & \overset{K_b}{\rightleftharpoons} & E \\ \downarrow k_x & & \downarrow k_n & & \\ H_2EA & & HEA & & \end{array}$$

Table III: Macroscopic pK Values and pH-Independent Rate Constants for Reactions of Native and Modified Enzymes[a]

reaction	k/K_{NAD}	k	k/K_{pyz}
E + NAD^+ + pyrazole	pK_a = 6.9 pK_b = 9.0 k_n = 2.4 μM^{-1} s^{-1}	pK_a = 7.6 k_x = 2500 s^{-1} k_n = 25 s^{-1}	pK_a = 7.1 pK_b = 10 k_x = 0.8 μM^{-1} s^{-1} k_n = 8.4 mM^{-1} s^{-1}
Im–E + NAD^+ + pyrazole[b]	pK_b = 9.9 k_n = 0.4 μM^{-1} s^{-1}	pK_a = 7.9 k_x = 1200 s^{-1} k_n = 38 s^{-1}	pK_a = 6.4 (0.4) pK_b = 9.5 k_x = 0.2 μM^{-1} s^{-1} k_n = 17 mM^{-1} s^{-1}
AI–E + NAD^+ + pyrazole[c]	pK_a = 6.7 k_n = 2.6 μM^{-1} s^{-1}	pK_a = 7.6 k_x = 1600 s^{-1} k_n = 32 s^{-1}	pK_a = 8.3 k_x = 0.2 μM^{-1} s^{-1} k_n = 7.9 mM^{-1} s^{-1}

reaction	k_{oxidn}	k/K_{PrOH}
E + NAD^+ + 1-propanol[d]	pK_a = 5.9 pK_b = 10 k_n = 320 s^{-1}	pK_a = 8.2 k_x = 0.7 μM^{-1} s^{-1}

[a] The logarithmic form of eq 2, which describes the pH dependence of kinetic constants according to Scheme IV, and its simplified forms were used to fit the pH dependence of kinetic constants and obtain their apparent pK values and pH-independent rate constants:

$$k_{obsd} = (k_n + k_x[H^+]/K_a)/(1 + K_b/[H^+] + [H^+]/K_a) \quad (2)$$

If $k_x = 0$, eq 2 reduces to

$$k_{obsd} = k_n/(1 + [H^+]/K_a + K_b/[H^+]) \quad (3)$$

When $K_b \ll [H^+]$, eq 2 simplifies to

$$k_{obsd} = (k_n + k_x[H^+]/K_a)/(1 + [H^+]/K_a) \quad (4)$$

When $K_a \gg [H^+]$ and $k_x = 0$

$$k_{obsd} = k_n/(1 + K_b/[H^+]) \quad (5)$$

Standard errors in estimation of pK values were usually 0.3 unit or better unless indicated otherwise in parentheses next to the pK value. Standard errors in estimation of k_n values for coenzyme association and k_x and k_n values for pyrazole binding were 20% or less, whereas the error in estimation of k_x for isomerization was as high as 50%. [b] Enzyme containing imidazole bound to the catalytic zinc. [c] Enzyme with acetimidylated ε-amino groups. [d] Saturating concentrations of NAD^+ were used for this set of experiments; hence, k/K_{NAD} could not be determined.

Factors That Control NAD^+ Binding. The kinetics of ternary complex formation with native enzyme, enzyme with imidazole bound to catalytic zinc, and acetimidylated enzyme were studied with the experimental design shown in Figure 1 at varied pH values. Figure 4A–C shows the pH dependencies of the first- and second-order kinetic constants for these enzymes. Apparent macroscopic pK values obtained for the mechanism in Scheme IV (where H_2E, HE, and E represent different protonated forms of enzyme, A is a ligand, and k_x and k_n are maximum and minimum rate constants) are listed in Table III.

The overall bimolecular rate constant for NAD^+ association shows a bell-shaped pH dependence for native enzyme with apparent pK values of 6.9 and 9.0 (Figure 4A). A pK of 9.2 has been reported by other workers for NAD^+ binding with native enzyme from stopped-flow kinetics, but to our knowl-

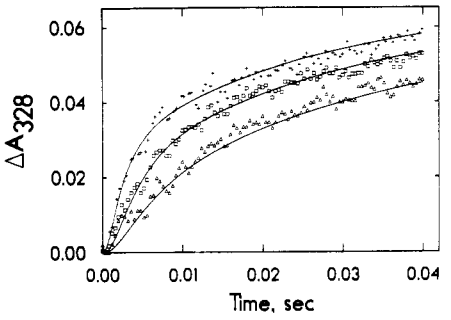

FIGURE 5: Kinetics of transient and steady-state oxidation of 1-propanol by NAD^+ and native enzyme in the stopped-flow spectrophotometer. Lines are simulated curves, and points are experimental. Native enzyme at 9.0 μN catalyzed the reaction of 2 mM NAD^+ and 0.5 mM propanol (△), 1.0 mM propanol (□), and 5.0 mM propanol (+) at 25 °C at pH 8. Rate constants obtained with FITSIM are listed in Table IV.

edge no evidence of a pK value less than 7 has been obtained (Detraglia et al., 1977; Kvassman & Pettersson, 1979; Pettersson, 1987). Steady-state kinetics, however, suggest a pK in this region (Dalziel, 1963). Displacement by imidazole of water bound to catalytic zinc abolished the pK at 6.9 (Figure 4B), whereas the pK at 9.0 was not observed for acetimidylated enzyme (Figure 4C).

The rate constants for the isomerization of enzyme–NAD^+ complex and pyrazole binding had apparent pK values of 7.6 and 7.1 for native enzyme (Figure 4A). Acetimidylation of ϵ-amino groups of lysine residues or coordination of imidazole to catalytic zinc did not abolish this pK (Figure 4B,C). A pK value of 7.6 was also reported for pyrazole binding to the native enzyme–NAD^+ complex (Andersson et al., 1981b). Another pK in the range 9.5–10 characterizes the pH dependence of pyrazole binding rate for native enzyme (Figure 4A) and the enzyme in which imidazole is bound to catalytic zinc (Figure 4B). Acetimidylated enzyme, however, does not exhibit a pK in this range for this rate constant (Figure 4C).

Transient Oxidation of 1-Propanol. Figure 4D shows the pH dependence of the observed maximum oxidation rate constant (k_{oxidn}) for 1-propanol and k/K_m (k_{on}) for the burst phase. Maximum rate constants at each pH were obtained by extrapolation of apparent rate constants to infinite propanol concentration at saturating NAD^+. pK values of 5.9 and 10.2 describe the effect of pH on the oxidation rate constant. A pK of 5.9 for the process is in good agreement with a pK of 6.4 observed for ethanol (Brooks et al., 1972) and benzyl alcohol (Kvassman & Pettersson, 1978) as substrates. However, the apparent pK at 10.2 has not been reported with these alcohols. k/K_m for propanol was fitted by an apparent pK of 8.2, which is comparable to the pK of 7.1 observed for pyrazole binding by enzyme–NAD^+ complex.

Progress curves for transient and steady-state phases of 1-propanol oxidation by NAD^+ and native enzyme in the stopped-flow instrument were fitted with FITSIM to a mechanism incorporating the isomerization of E–NAD^+ complex (Scheme I). Figure 5 shows that the data can be simulated well. The rate constants determined for the overall mechanism for native enzyme are given in Table IV.

Table IV: Rate Constants for Oxidation of 1-Propanol Catalyzed by Native Enzyme[a]

$$*\text{E–NAD}^+ \underset{k_{-3}}{\overset{k_3,\ \text{Alc}}{\rightleftharpoons}} \text{E–NAD–Alc} \underset{k_{-4}}{\overset{k_4}{\rightleftharpoons}} \text{E–NADH–Ald} \underset{k_{-5},\ \text{Ald}}{\overset{k_5}{\rightleftharpoons}}$$

$$\text{E–NADH} \underset{k_{-6}\ \text{NADH}}{\overset{k_6}{\rightleftharpoons}} \text{E}$$

rate constant	value	rate constant	value
k_3 (M^{-1} s^{-1})	4.5×10^5	k_{-4} (s^{-1})	2500
k_{-3} (s^{-1})	88	k_5 (s^{-1})	55
k_4 (s^{-1})	1400	k_{-5} (M^{-1} s^{-1})	6.1×10^6

[a] These rate constants were estimated by fitting the stopped-flow time courses for oxidation of varying concentrations of 1-propanol by 2 mM NAD^+ and 9 μN native enzyme, with the program FITSIM. Values for k_1, k_{-1}, k_2, and k_{-2} are listed in Table II and were fixed in these simulations. Experimentally determined values for NADH off-rate constant (k_6) and on-rate constant (k_{-6}), which are 5.5 s^{-1} and 1.1×10^7 M^{-1} s^{-1}, respectively, at pH 8 and 25 °C, were also fixed. Standard errors in estimation of rate constants were 20% or less.

Scheme V

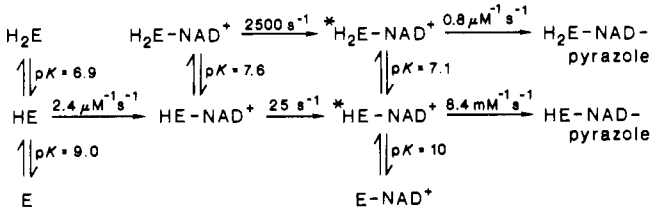

protein changes conformation upon binding NAD^+ and a substrate or substrate analogue (Eklund et al., 1976; Eklund & Brändén, 1987). Our results do not rule out further isomerizations of ternary complexes.

Estimated rate constants for NAD^+ binding (Table II) suggest that the coenzyme associates at a diffusion-controlled limit (about 10^8 M^{-1} s^{-1}) and then binary complex isomerizes (500 s^{-1} at pH 8). It has been postulated that the adenosine monophosphate moiety of NAD^+ controls the rate of NAD^+ binding and the nicotinamide mononucleotide moiety controls its dissociation rate (Shore, 1969; Shore & Gilleland, 1970). Thus, the isomerization step may involve the repositioning of the nicotinamide ring in the active site. Hardman (1981) proposed that the dissociation of NAD^+ is limited by the conformational change from closed to open form. This may involve the movement of the nicotinamide moiety away from the active site followed by the rapid dissociation of the adenosine monophosphate moiety. The observed rate constant for dissociation of NAD^+ from *E–NAD^+ complex is expressed by $k_{off} = k_{-1}k_{-2}/(k_{-1} + k_2)(k_2 + k_{-2})$. This value is about 90 s^{-1} when the estimated values for k_{-1}, k_2, and k_{-2} (Table II) are substituted in the above expression, which is higher than the turnover number at pH 8, 25 °C (47 s^{-1}), with acetaldehyde (Dalziel, 1963).

pH Dependence of Kinetic Constants. The effect of pH on kinetic constants of native enzyme has been intensively investigated, yet it is still unclear which amino acid residues are responsible for the observed pH dependencies of coenzyme association and dissociation, substrate binding, and hydrogen-transfer steps. Functional groups in the active site that can ionize in the pH range examined are the zinc-bound water, the imidazolium moiety of His-51, and the ϵ-ammonium group of Lys-228. Scheme V summarizes the pK values and pH-independent kinetic constants for native enzyme.

Native and acetimidylated enzymes react faster with NAD^+ after deprotonation of a group with a pK of 6.7–6.9. Displacement of zinc-bound water with imidazole abolishes this dependence, implying that the pK may originate from the

DISCUSSION

NAD^+ Binding and Conformational Change. Although the limiting rates observed for the formation of ternary complex can be explained in various ways, we think that the mechanism in Scheme I best describes the results. Isomerization of the enzyme–NAD^+ complex is consistent with the X-ray crystallography of apo- and holoenzyme, which suggests that the

water molecule. It is not likely, however, that this water molecule has such a low microscopic pK because the catalytic zinc has an overall zero charge by virtue of its binding to the negatively charged thiolates of Cys-46 and Cys-174. Furthermore, a pK of 6.9 is close to the value expected for the imidazolium moiety of histidine. We think that this is a macroscopic pK for the hydrogen-bonded system that extends from the zinc–water to the imidazole nitrogen of His-51 through the hydroxyl group of Ser-48 and a solvent molecule:

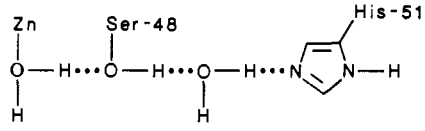

In holoenzyme, the water molecule is replaced by the 2′-hydroxyl group of the nicotinamide ribose, as shown by crystallography (Eklund et al., 1982a). Since the nicotinamide of NAD^+ is positively charged, deprotonation of the imidazolium moiety in the hydrogen-bonded system may decrease repulsion between these like-charged moieties and accelerate the association of coenzyme. Moreover, a hydrogen bond between the ribose hydroxyl group and the imidazole nitrogen of His-51 can be strengthened by deprotonation of this nitrogen. Upon displacement of zinc-bound water with imidazole, this hydrogen-bonded system could be disrupted and the pK of His-51 shifted to a value below 6. Alternatively, the bulky imidazole on the zinc could have decreased the NAD^+ association rate to such an extent that the system is no longer sensitive to the effects of ionization of His-51.

As indicated above, the rate of coenzyme association is controlled by another functional group with a pK of 9.0 for native enzyme, with the rates being faster below this pK. Enzyme complexed with imidazole also exhibits a pK of 9.9 for this process, which agrees with the pK of 9.8 obtained from fluorescence titration (Parker et al., 1978). If zinc–water were responsible for this pK, it should have been abolished when imidazole displaced the water. Acetimidylated enzyme, however, does not show a pK at 9 for this process, but the data may be described with a pK at 11. Thus, acetimidylation either abolishes this pK or shifts it by 2 pH units, which is about the same as the difference between the pK values of lysine and acetimidyllysine. The pyrophosphate group of NAD^+ binds to the guanidinium groups of Arg-47 and Arg-369, but Lys-228 also interacts electrostatically. We therefore assign the pK of 9 on native enzyme to the ϵ-amino group of Lys-228. The positively charged Lys-228 best attracts the negatively charged pyrophosphate of NAD^+.

All three enzymes studied exhibit an apparent pK in the range of 6.4–8.3 for pyrazole binding and for isomerization of binary complexes, with the rates being faster below this pK for both steps. Neither zinc–water nor the ϵ-amino group of Lys-228 can be this functional group because the enzymes with imidazole bound to zinc and acetimidylated lysines also show this pH dependence. Our results do not agree with the assignment made by other workers that zinc–water is responsible for this pK (Andersson et al., 1981b; Pettersson 1987). We suggest that His-51 controls the isomerization and pyrazole binding steps. As discussed earlier, the imidazole of His-51 is hydrogen bonded to zinc–water through hydroxyl groups of nicotinamide ribose and Ser-48, making this a macroscopic pK rather than a microscopic pK of one group. When the proton on imidazolium is lost, this system becomes neutral and may become zwitterionic, giving hydroxide character to zinc–water and a partial positive charge on the imidazole. In order for pyrazole to bind to zinc, the water molecule must be displaced, and it is well-known that dissociation of water from a metal ion is faster than the dissociation of hydroxide ion. The observed decrease in pyrazole binding rate constants above this pK can be explained on this basis. It is likely that the amino acid with a pK value about 10 that controls pyrazole binding for native and imidazole-bound enzymes is Lys-228 as acetimidylation abolishes this pK. The interaction of Lys-228 with the pyrophosphate group of the coenzyme would be reflected by an upward shift of its pK in the holoenzyme.

The isomerization of E–NAD^+ complex is postulated to be important for proper positioning of amino acid residues in the active site. It is reasonable to assume that the isomerization of the binary complex also involves the incorporation of the ribose hydroxyl group into the hydrogen-bonded system, as this serves in proton relay during catalysis (Hennecke & Plapp, 1983). The solvent molecule between the hydroxyl group of Ser-48 and the imidazole of His-51 must be replaced by the hydroxyl group of the nicotinamide ribose. Upon deprotonation of the His-51 imidazole, the hydrogen bond between this water molecule and the imidazole moiety will be strengthened, thereby making the removal of the solvent molecule more difficult and slower. Our results agree with the above argument as there is a decrease in the isomerization rate constant above a pK of about 7.6.

Isomerization and Catalytic Reaction. For the transient oxidation of ethanol and benzyl alcohol, a pK of 6.4 has been assigned to zinc-bound alcohol (Kvassman & Pettersson, 1978). We found a similar pK of 5.9 for propanol oxidation. Although this pK may reflect the zinc-bound alcohol, it is probably a macroscopic pK for the hydrogen-bonded system, which transfers a proton to solvent. A downward shift of 1–1.5 units in the ternary complex as compared to that of the binary complex can be explained by the difference in the pK values of water and alcohol, as this pK is for the coupled system. The functional group that has a pK of 10.2 and ionizes to decrease the oxidation rate is tentatively assigned to the ϵ-amino group of Lys-228. The pK value of 8.2 that characterizes the observed pH dependence of k/K_m for propanol is attributed to the hydrogen-bonded system.

Computer simulations suggest that the rate constant (k_4 in Table IV) for hydride transfer from propanol to NAD^+ is 1400 s^{-1}, whereas the observed maximum rate constant for transient oxidation of propanol at pH 8 is about 310 s^{-1}. It is apparent that the isomerization is a major limiting step in alcohol oxidation. The observed rate constant for this process can be calculated by use of the expression $k_{obsd} = k_2k_4/(k_2 + k_4)$, which is about 370 s^{-1} with the values estimated from FITSIM for k_2 and k_4. Thus, for good substrates the hydride transfer rate could be limited by the binary complex isomerization. The characterization of this additional step in the mechanism is therefore crucial for understanding the catalytic reaction.

ACKNOWLEDGMENTS

We thank Drs. C. T. Zimmerle and C. Frieden for providing the KINSIM/FITSIM programs and for assistance in using them.

REFERENCES

Andersson, P., Kvassman, J., Lindström, A., Oldén, B., & Pettersson, G. (1981a) *Eur. J. Biochem. 113*, 425–433.

Andersson, P., Kvassman, J., Lindström, A., Oldén, B., & Pettersson, G. (1981b) *Eur. J. Biochem. 114*, 549–556.

Barshop, B. A., Wrenn, R. F., & Frieden, C. (1983) *Anal. Biochem. 130*, 134–145.

Brooks, R. L., Shore, J. D., & Gutfreund, H. (1972) *J. Biol. Chem. 247*, 2382–2383.

Cleland, W. W. (1979) *Methods Enzymol. 63*, 103–138.

Coates, J. H., Hardman, M. J., Shore, J. D., & Gutfreund, H. (1977) *FEBS Lett. 84*, 25–28.
Colonna-Cesari, F., Perahia, D., Karplus, M., Eklund, H., Brändén, C.-I., & Tapia O. (1986) *J. Biol. Chem. 261*, 15273–15280.
Dalziel, K. (1963) *J. Biol. Chem. 238*, 2850–2858.
Dalziel, K., & Dickinson, F. M. (1966) *Biochem. J. 100*, 491–500.
Detraglia, M. C., Schmidt, J., Dunn, M. F., & McFarland, J. T. (1977) *J. Biol. Chem. 252*, 3493–3500.
Dunn, M. F., Bernhard, S. A., Anderson, D., Copeland, A., Morris, R. G., & Roque, J.-P. (1979) *Biochemistry 18*, 2346–2354.
Eklund, H., & Brändén, C.-I. (1987) *Active Sites of Enzymes* (Jurnak, F. A., & McPherson, A. Eds.) pp 73–142, Wiley, New York.
Eklund, H., Samama, J.-P., Wallén, L., Brändén, C.-I., Åkeson, Å., & Jones, T. A. (1976) *J. Mol. Biol. 102*, 27–59.
Eklund, H., Samama, J.-P., Wallén, L., Brändén, C.-I., Åkeson, Å., & Jones, T. A. (1981) *J. Mol. Biol. 46*, 561–587.
Eklund, H., Plapp, B. V., Samama, J.-P., & Brändén, C.-I. (1982a) *J. Biol. Chem. 257*, 14349–14358.
Eklund, H., Samama, J.-P., & Wallén, L. (1982b) *Biochemistry 21*, 4858–4866.
Eklund, H., Samama, J.-P., & Jones, T. A. (1984) *Biochemistry 23*, 5982–5996.
Frolich, M., Creighton, D. J., & Sigman, D. S. (1978) *Arch. Biochem. Biophys. 189*, 471–480.
Gilleland, M., & Shore, J. (1970) *Biochem. Biophys. Res. Commun. 40*, 230–235.
Hardman, M. J. (1981) *Biochem. J. Lett. 195*, 773–774.
Hennecke, M., & Plapp, B. V., (1983) *Biochemistry 22*, 3721–3728.
Kvassman, J., & Pettersson, G. (1978) *Eur. J. Biochem. 87*, 417–427.
Kvassman, J., & Pettersson, G. (1979) *Eur. J. Biochem. 100*, 115–123.
Oldén, B., & Pettersson, G. (1982) *Eur. J. Biochem. 125*, 311–315.
Parker, D. M., Hardman, M. J., Plapp, B. V., Holbrook, J. J., & Shore, J. D. (1978) *Biochem. J. 173*, 269–275.
Pettersson, G. (1987) *CRC Crit. Rev. Biochem. 21*, 349–389.
Plapp, B. V., Brooks, R. L., & Shore, J. D. (1973) *J. Biol. Chem. 248*, 3470–3475.
Plapp, B. V., Eklund, H., & Brändén, C.-I. (1978) *J. Mol. Biol. 122*, 23–32.
Plapp, B. V., Sogin, D. C., Dworschack, R. T., Bohlken, D. P., Woenckhaus, C., & Jeck, R. (1986) *Biochemistry 25*, 5396–5402.
Samama, J.-P., Zeppezauer, E., Biellmann, J.-F., & Brändén, C.-I. (1977) *Eur. J. Biochem. 81*, 403–409.
Shore, J. D. (1969) *Biochemistry 8*, 1588–1590.
Shore, J. D., & Gilleland, M. J. (1970) *J. Biol. Chem. 245*, 3422–3425.
Sigman, D. S. (1967) *J. Biol. Chem. 242*, 3815–3824.
Theorell, H., & Bonnichsen, R. (1951) *Acta Chem. Scand. 5*, 1105–1126.
Theorell, H., & Yonetani, T. (1963) *Biochem. Z. 338*, 537–553.
Theorell, H., Yonetani, T., & Sjöberg, B. (1969) *Acta Chem. Scand. 23*, 255–260.
Tonomura, B., Nakatani, H., Ohnishi, M., Yamaguchi-Ito, J., & Hiromi, K. (1978) *Anal. Biochem. 84*, 370–383.
Wolfe, J. K., Weidig, C. F., Halvorson, H. R., Shore, J. D., Parker, D. M., & Holbrook, J. J. (1977) *J. Biol. Chem. 252*, 433–436.
Wratten, C. C., & Cleland, W. W. (1963) *Biochemistry 2*, 935–941.
Zimmerle, C. T., Patane, K., & Frieden, C. (1987) *Biochemistry 26*, 6545–6552.